

Melt rheology of poly(lactic acid): Entanglement and chain architecture effects

John R. Dorgan^{a)} and Joshua S. Williams

*Department of Chemical Engineering, Colorado School of Mines,
Golden, Colorado 80401*

David N. Lewis

Chronopol Inc., 4545 McIntyre Street, Golden, Colorado 80403

(Received 23 September 1998; final revision received 25 June 1999)

Synopsis

Poly(lactic acids) (PLAs) are a family of polyesters available via fermentation from renewable resources and are the subject of considerable recent commercial attention. In this study, the melt rheological properties of a family of poly(lactic acid) stars are investigated and compared to the properties of the linear material. For polymers made from a 98:2 ratio of the *L* to *D* enantiomeric monomers it is found that the entanglement molecular weight is in the range of 9000 g per mole ($M_e \approx 8700$ g/mol) while the molecular weight for branch entanglement is inferred to be approximately 3500 g per mole ($M_b \approx 34\,600$ g/mol). In addition, the zero shear viscosity of the linear material increases with the 4.6 power of molecular weight. These results may suggest that PLA is a semistiff polymer in accordance with other recent findings. The increase in zero shear viscosity for the branched materials is measured and quantified in terms of appropriate enhancement factors. Relaxation spectra show that the transition zone for the linear and branched materials are nearly indistinguishable, while the star polymers have greater contributions to the terminal regime. The effects of chain architecture on the flow activation are found to be modest, implying that small scale motions in PLA homopolymers largely control this phenomenon. Good agreement is found between the dynamic data and many aspects of the theory of star polymers, however, a dependence of the zero shear viscosity on the number of arms is observed. © 1999 The Society of Rheology. [S0148-6055(99)01305-X]

I. INTRODUCTION

A. Importance

Poly(lactic acid) (PLA) is not a new material. The polymer of lactic acid has been known for many years. [Flory (1953)]. However, despite relatively good mechanical properties, PLA never received much attention due to its high cost of production. Recent interest in PLA stems in part from its degradability; several interesting applications are possible with degradable polymers. In addition, recent advances in fermentation technology mean that PLA appears to be economically viable in many markets [Datta *et al.* (1995)].

^{a)}Author to whom correspondence should be addressed; electronic mail: jdorgan@mines.edu

An interesting aspect of PLA is its availability from monomers produced by the fermentation of agricultural crops and waste products. The availability of PLA from agricultural feedstocks, rather than fossil fuels, means that its use produces a net zero contribution to CO₂ emissions (the carbon present is fixed by photosynthesis and comes from the atmosphere). Due to these “green” features combined and its benign degradation behavior, PLA is attracting attention as a potential packaging material. Some cost estimates place PLA at less than \$1.00 lb. thus making it an economically realistic packaging material [Thayer (1997)].

PLA is also an extremely important biomaterial. The biomedical uses of PLA are widespread and include bioabsorbable surgical sutures and implants [Reed and Gilding (1981); Taylor *et al.* (1994)] as well as matrices for both controlled drug delivery [Jalil (1990); Park *et al.* (1992); Sampath *et al.* (1992); Sturesson *et al.* (1993); Park *et al.* (1994)] and tissue culturing [Mikos *et al.* (1994); Kohn (1996)]. These applications generally rely on the hydrolytic degradation of PLA which can be controlled in a number of ways including blending, degree of crystallization, and through copolymerization [Siparsky *et al.* (1997)]. Hydrolysis of the ester bonds produces lactic acid, a nontoxic and naturally occurring metabolite.

Finally, PLA is interesting purely in terms of having good mechanical properties for a potentially inexpensive material. For example, Leenslag and Pennings report a tensile modulus of 14 GPa (2 Mpsi) for solution spun PLA fibers [Leenslag and Pennings (1987)].

B. Previous studies

Despite the considerable interest in and work on PLA, no comprehensive studies of the melt rheological properties are yet available in the open literature. One noteworthy study is that of Witzke and co-workers that summarizes many of the physical properties of PLA and provides some rheological data on linear architectures [Witzke (1997)]. Work on mechanical properties in the solid state has opened up a variety of technologically important and scientifically interesting issues surrounding the mechanical response of PLAs. In particular the value of C_∞ (a fundamental chain property defined as the ratio of the chain dimensions under theta conditions to the size of a random walk) is in dispute. Work by Pennings and co-workers on PLA points to a C_∞ value in the vicinity of 9–12, [Grijpma *et al.* (1994); Cornelis *et al.* (1996)] rather than the value of 2.0+/-0.2 reported by Flory [Tonelli and Flory (1969); Tonelli *et al.* (1969)]. If PLA is a very flexible chain characterized by a low C_∞ value then it is expected that it should fail in a ductile fashion rather than in the brittle manner that is observed. The high C_∞ values now associated with PLA mean that it is expected to assume extended chain conformations leading to a relatively large value for the molecular weight between entanglements (M_e). Based on measurements of the plateau modulus in PLA, Pennings reports a value of $M_e = 10\,500$ g/mol at 200 °C [Grijpma *et al.* (1994)].

C. Present work

In this investigation, several rheological features of PLA homopolymers are presented for the first time. The effects of chain architecture in the form of branching are studied in a series of homopolymers consisting of two-arm (i.e., linear), four-arm, and six-arm poly(lactic acid) stars. Solid-state mechanical properties for PLA star polymers have been previously reported by Spinu and co-workers. [Spinu *et al.* (1996)]. The limits of linear viscoelasticity are determined and time-temperature superposition is performed to provide master flow curves and activation energies. Results for the zero shear viscosity

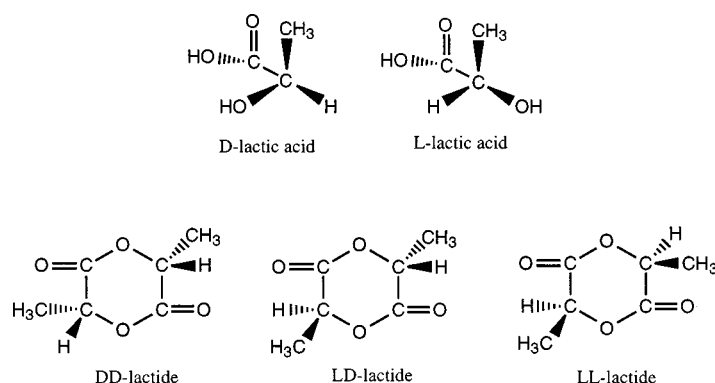


FIG. 1. Stereochemistry of lactic acid and its lactide rings.

versus molecular weight for all three types of architectures are presented and analyzed in terms of appropriate enhancement factors. Measurements of the plateau modulus are used to determine a value of the molecular weight between entanglements M_e and the zero shear data is used to infer a value for the molecular weight for branch entanglement M_b . The effects of branching, by use of the star architecture, on shear viscosity and molecular dynamics are investigated.

II. MATERIALS AND METHODS

A. Synthesis and isolation methods

Due to the chiral nature of lactic acid, the stereochemistry of PLAs is complex. Figure 1 shows the *L* and *D* enantiomers of lactic acid along with its possible dimer rings. It is these lactide rings which are used as the monomer in producing the PLAs of this study. Control of the ratio of *L* to *D* monomer content is an important molecular feature of PLAs. Polymerization of the pure *LL*-lactide or the *DD*-lactide produces completely syndiotactic materials (which are the mirror images of each other). Mixing of these monomeric forms produces a polymer in which the strict stereoregularity is disrupted. *L*-lactic acid is available from fermentation and so the *LL*-lactide is of greatest commercial interest.

All polymers were synthesized in the melt using stannous octoate as a catalyst. The lactide monomers were charged in a 98:2 *LL*:*DD* ratio into a Haake Rheodyne 5000 mixing bowl and polymerizations were conducted at 180 °C. Linear PLAs (two-arm) were initiated with 1,4 butanediol, four arm by 2,2, hydroxymethyl 1,3 propanediol, and six arm by 1,2,3,4,5,6 hexahydroxyhexane. Acetic anhydride was added in slight excess to convert the alcohol groups on the chain ends to nonreactive species.

PLA was dissolved in dichloromethane to make a 10 wt% solution that was subsequently added to a 50:50 by weight mixture of dichloromethane and methanol. Precipitation was aided by adding additional methanol as needed until the polymer could be filtered off as a white fibrous material. Materials were then dried overnight in a vacuum oven at 50 °C and 10 in. of water vacuum. For dynamic testing, disks were vacuum molded at 180 °C and again dried at 50 °C overnight in a vacuum oven.

B. Testing methods

Molecular weight measurements were performed by combined light scattering and gel permeation chromatography to give absolute values for the weight M_w and number M_n

TABLE I. Sample designations and molecular weight characteristics.

Sample	Nominal M_w	Post test M_w	p
DI 260	260 k	246 k	1.57
DI 210	210 k	210 k	1.57
DI 199	199 k	156 k	1.47
TI 260	260 k	227 k	1.71
TI 199	199 k	199 k	1.50
TI 156	156 k	163 k	1.36
HI 280	280 k	251 k	1.63
HI 213	213 k	208 k	1.51
HI 147	147 k	159 k	1.22

averaged molecular weights. Molecular weights were measured for the samples recovered after rheological testing.

Table I is a summary of the PLA materials tested. The nominal weight average molecular weight is calculated from the ratio of monomer to initiator assuming no polydispersity. The post test weight average molecular weight is a measured quantity. The polydispersity is reported for the post test samples in terms of the measured polydispersity index ($p = M_w/M_n$). Note that the ring opening addition polymerization produces materials with dispersities less than the equilibrium value of 2.0 associated with step polymerizations; any water present will lead to a redistribution in the molecular weight distribution.

Dynamic moduli and viscosities were measured in a Rheometrics RMS-605 running RHIOS and RHECALC software packages. A special pressure canister containing molecular sieves and drierite was installed in the inlet air line to the oven in order to exclude moisture and minimize hydrolytic degradation during testing. Measurements were again taken starting at high shear rates and working towards low shear rates.

III. RESULTS

A. Dynamic testing

For each material investigated the limits of linear viscoelasticity were determined by performing strain sweeps at a series of fixed frequencies. In such tests the storage modulus ($G'(\omega)$) remained constant at low strains but decreased at larger values of the strain indicating a nonlinear response. The limit of linear viscoelasticity is taken as the point at which the storage modulus decreased by 5% from its low strain plateau value.

The rheometer was programmed to perform frequency sweeps from 500 (1/s) down to 0.05 (1/s) at strains which lie well within the linear deformation limits for the respective frequency and temperature. Data were generated for the three chain architectures at temperatures of 170, 180, and 190 °C. These data made time–temperature superposition possible and a reference temperature of 180 °C was chosen as most representative of a typical processing temperature. The complex viscosity versus shear rate was fit to the Carreau model using the Rheometrics RHECALC software package in order to determine zero shear viscosities.

Figures 2–4 present the dynamic spectra for the highest molecular weight diol (two-arm), tetrol (four-arm), and hexol (six-arm) initiated star polymers. Several interesting features of the rheological response of these materials are evident. All of the polymers exhibit a clear zero shear viscosity followed by a shear thinning region. Here it is noted only that the zero shear viscosity and the shear thinning both increase with the addition of

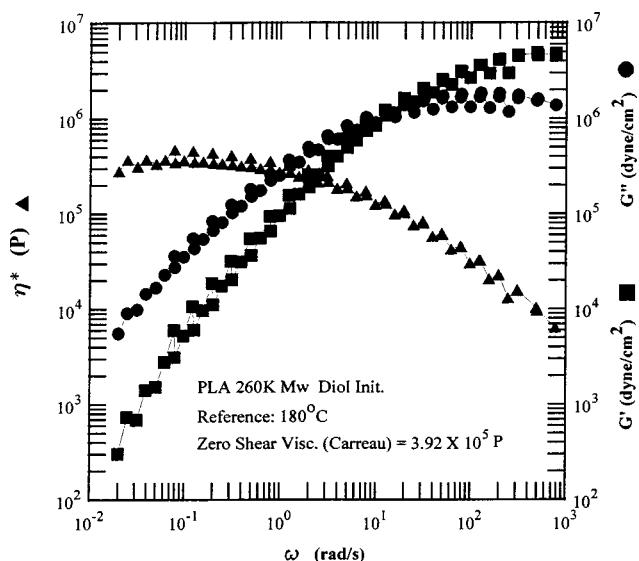


FIG. 2. Linear viscoelastic spectra for a diol initiated 98:2 *L:D* PLA.

branching. It is also noteworthy that in the case of the linear polymer a clearly evidenced maximum in the $G''(\omega)$ spectra is exhibited shortly after the crossover point [where $G'(\omega) = G''(\omega)$] while the branched materials exhibit no such maxima in the available frequency region. A more detailed analysis of the dynamics is in Sec. IV.

Table II lists Arrhenius flow activation energies for the zero shear viscosities referred to the measurement temperatures. While the temperature range is narrow by normal commodity polymer standards, it is seen that there is little difference between the activation energies as a function of chain architecture. This result suggests that the flow

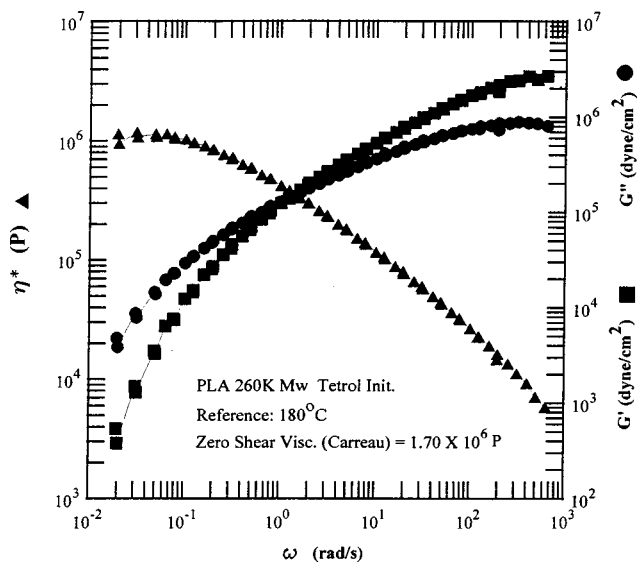


FIG. 3. Linear viscoelastic spectra for a tetrol initiated 98:2 *L:D* PLA.

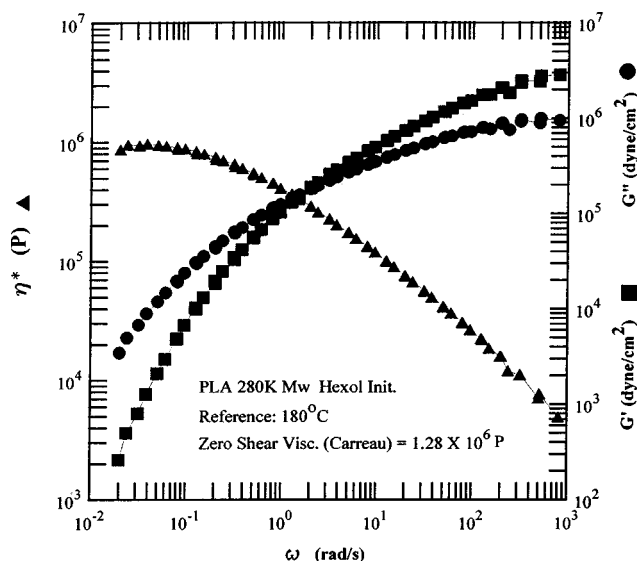


FIG. 4. Linear viscoelastic spectra for a hexol initiated 98:2 *L:D* PLA.

activation energy is affected only by small scale local motions of the polymer chain rather than by large scale self-diffusive motions.

Additional information about local versus long range molecular motions is available by considering the relaxation spectra of the different chain architectures. Figure 5 displays a comparison of the relaxation spectra for a six-arm star polymer to the linear chain calculated from the dynamic data at 180 °C. It is apparent that the spectra are nearly identical for fast relaxation times (milliseconds and less) but diverge greatly for larger relaxation times. This finding is in agreement with the hindered reptation theory of Pearson and Helfand for the dynamics of star polymers. [Pearson and Helfand (1984)]. Further comparison of the data and theory appears in Sec. IV.

IV. DISCUSSION

Given the pending importance of the PLA family and the paucity of rheological data available in the open literature, several important issues can be addressed by the present study. Primarily, the interest is in characterizing some of the very fundamental properties of PLA. These include, but are not limited to, the entanglement molecular weight M_e and

TABLE II. Flow activation energies (J/mol K) for PLA samples of varying chain architecture and molecular weight

Sample	170 °C	180 °C	190 °C
DI 260	8.62×10^4	9.20×10^4	9.35×10^4
DI 199	7.82×10^4	7.98×10^4	8.13×10^4
TI 260	9.82×10^4	1.04×10^5	9.86×10^4
TI 199	1.43×10^4	1.56×10^5	1.63×10^5
TI 156	9.57×10^4	1.08×10^5	1.12×10^5
HI 280	9.56×10^4	1.01×10^5	1.02×10^5
HI 213	1.13×10^5	1.16×10^5	1.20×10^5
HI 147	9.38×10^4	9.32×10^4	9.93×10^4

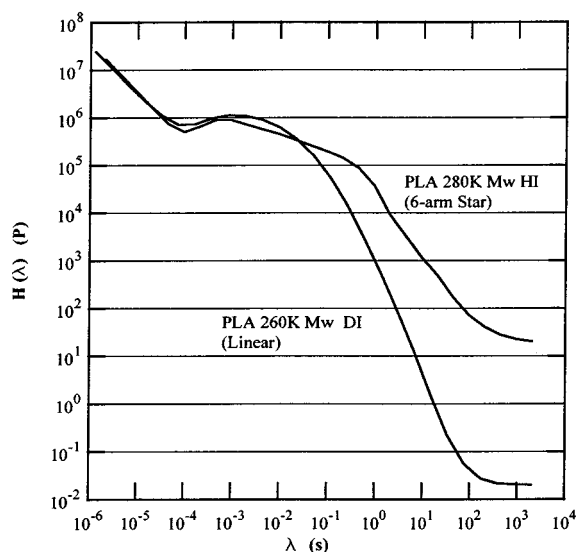


FIG. 5. Comparative relaxation spectra of a six-arm star to a linear PLA. Fast relaxations associated with local chain motions are indistinguishable but long time motions are severely altered by the molecular architecture.

the molecular weight for branch entanglement M_b . These quantities along with the scaling of the zero shear viscosity with molecular weight gives an indication of the chain stiffness. The effects of branching are of vital importance and the dynamics of the star architecture is a topic of interest in and of itself. Each of these topics is addressed in this section.

A. Effects of branching

Branching is often introduced to modify the flow properties of polymeric materials for specific forming operations. The general effects associated with branching are reasonably well understood [Dealy and Wissbrun (1990)]. For comparable molecular weights, it is generally found that the zero shear viscosity *decreases* as short chains are added to a polymer backbone. The reason for these phenomena is that the overall size (as measured for example by the molecular radius of gyration) is decreased. It is only when the branch length exceeds some critical value that the branches themselves entangle and lead to an *increase* in the viscosity for a comparable molecular weight. At higher shear rates the viscosity of the long branched material may actually be less than the linear material.

Figure 6 shows a direct comparison of the flow curve for the linear and four-arm star architectures of PLA for the same nominal molecular weight. The expected behavior for a material with long branches is evident. Namely, the zero shear viscosity is increased but the high shear rate values of viscosity are actually reduced. This type of flow behavior is advantageous for certain processing operations.

B. Plateau modulus and entanglement molecular weight

The plateau modulus G_n^0 of the various linear PLAs is available from the dynamic data. The Rheometrics RHECALC software package fits data in the following relationship where c_1 and c_2 are constants to calculate G_n^0 :

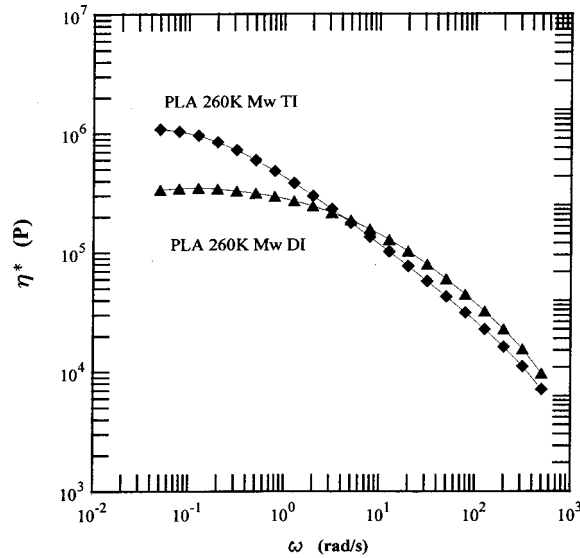


FIG. 6. Comparison of the flow curves for highly branched (four-arm star) and linear PLA.

$$G'(\omega) = G_n^0 + \left(\frac{c_1}{\omega^{c_2}} \right) \quad (1)$$

and provides values of between 3.3×10^6 and 6.5×10^6 (dyne/cm²). If instead the plateau modulus is calculated from G_c [the crossover modulus, where $G'(\omega) = G''(\omega)$] and the polydispersity index p according to the relationship proposed by Wu [Wu (1989)]

$$\log(G_n^0/G_c) = 0.38 + \frac{2.63 \log(p)}{1 + 2.45 \log(p)}, \quad (2)$$

the values are between 6.1×10^6 and 8.3×10^6 (dyne/cm²). Taking into consideration the spread of these values, the plateau modulus is here assigned a value of approximately $G_n^0 \approx 5.0 \times 10^6$ (dyne/cm²).

Calculation of the entanglement molecular weight proceeds according to Eq. (2) [Ferry (1980)]

$$M_e = \frac{\rho RT}{G_n^0}, \quad (3)$$

where ρ is the density, T is the temperature, and R is the gas constant. Using a measured density of 1.16 g/cm³ for PLA at 180 °C, the value for the molecular weight between entanglements is found to be $M_e \approx 8700$ g/mol. This value compares favorably with the 10 500 g/mol reported at 200 °C based on plateau values of a PLA having a L:D ratio of 85:15 by Pennings and co-workers [Grijpma *et al.* (1994)]. It should be noted that the range of plateau moduli estimated from the data correspond to values for the entanglement molecular weight ranging from 5700 to 14 400. However, the values of between 22 000 and 100 000 g/mol, depending on the catalyst used and the polymerization temperature, reported by Pennings and Grijpma for a 100:0 L:D ratio appear very large in comparison [Grijpma and Pennings (1994)]. There is of course some difficulty in assigning an exact value to the plateau modulus, particularly for polydisperse samples. In

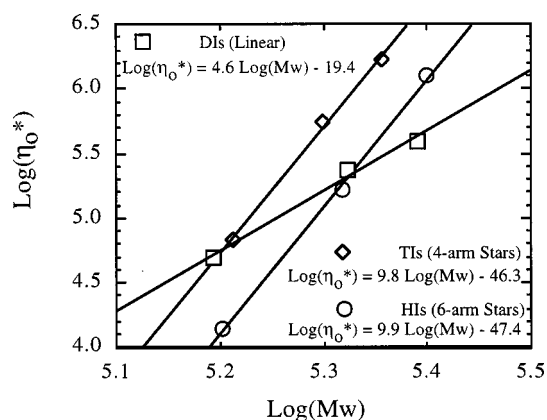


FIG. 7. Branching effects for poly(lactic acid) on the scaling of the complex zero shear viscosity with molecular weight.

addition, the complex stereochemical nature of the PLA chain must be remembered. Nonetheless, the existing data suggests that the entanglement molecular weight for the present 98:2 PLA is in the vicinity of 9000 g/mol.

C. Zero shear viscosity scaling with molecular weight

The scaling of viscosity with molecular weight (MW) is one of the long-standing issues in polymer rheology. The complex viscosity versus shear rate is fit to the Carreau model using the Rheometrics RHECALC software package in order to determine complex zero shear viscosities. Figure 7 shows the relationships between these zero shear viscosities and the weight averaged molecular weights for each of the three polymer architectures. Several interesting features are present in these results. First, the observed slope for the linear material is 4.6 rather than the usually 3.4 observed for truly random materials. This observation is consistent with the high C_∞ values measured by Pennings and is in qualitative agreement with other recent results on PLAs [Wang *et al.* (1997)]. However, if the lowest MW is reduced by 10% and the higher two MWs are increased by 10%, the slope falls to 3.2. The strong scaling exponent must be viewed with a degree of skepticism given the usual uncertainty in molecular weight measurements and the fact that all of the data fall roughly within 1 order of magnitude in MW. Witzke reports the 3.4 power expected for random chains in his study of PLAs [Witzke (1997)]. Figure 7 does show the expected result of the branched viscosity being lower than the linear architecture for the low molecular weight materials but higher for larger molecular weights.

The zero shear results of Fig. 7 may also be used to estimate a molecular weight for branch entanglement M_b from the intersection of the branched material curves with the linear material curve. This is because of the aforementioned fact that the viscosity of a branched material is less than a linear material of comparable molecular weight until the branch lengths reach the critical entanglement length M_b . Thereafter the viscosity of the branched material becomes greater. This reasoning implies that the intersection of the linear and branched material zero shear viscosities represents the point at which the branch length has reached a critical length. It is for this reason that the six-arm polymer intersects at a higher total molecular weight. Applying this reason to the tetrol initiated (four-arm) material yields a value for the branch entanglement molecular weight of $M_b \approx 37\,200$ g/mol while the hexol (six-arm) intersection gives $M_b \approx 32\,000$ g/mol. This

agreement is reasonable considering the limited scope of the data and the arithmetic average provides the value $M_b \approx 34\,600$ g/mol. Given that the approximate values for M_b and M_e are 35 000 and 9000 g/mol, the relationship $M_b \approx 4M_e$ is proposed.

D. Viscosity enhancement

The increase in viscosity for long branches can be described by enhancement factors. Here, the arguments put forth by Graessley are invoked [Graessley (1977)]. For short branch analogs, the viscosity depends only on molecular size. This means that the viscosity of a branched material η_B , should be equal to the viscosity of a linear analog η_L of the same size

$$\eta_B(M) = \eta_L(gM), \quad (4)$$

where g is the ratio of the mean square radius of gyration of the branched material to that of the linear material (i.e., $g = \langle S_B^2 \rangle / \langle S_L^2 \rangle$). Because the branched material has a smaller radius for a given molecular weight, it has a smaller viscosity.

For larger molecular weights, the branches themselves can entangle and the viscosity of the branched material can become much greater than the linear material. In this case it is convenient to define a “viscosity enhancement factor,” Γ , according to

$$\Gamma = \frac{\eta_B(M)}{\eta_L(gM)}. \quad (5)$$

This factor is unity at low values of the molecular weight but increases rapidly with increasing branch length. For star architectures, the ratio of radii can be estimated using the theoretical result of Zimm and Stockmayer

$$g = \frac{3f-2}{f^2}, \quad (6)$$

where f represents the functionality of the star (that is, the number of arms).

From the perspective of engineering a material with a prescribed zero shear viscosity, understanding the viscosity enhancement as a function of branch length is important. A particularly useful nondimensionalization for measuring the branch length is in terms of the number of entanglement strands; an entanglement strand is simply the length of the chain corresponding to the entanglement molecular weight. For a star polymer, the number of entanglement strands is trivial to calculate. Division of the total molecular weight M by the functionality f gives the molecular weight of a branch; dividing this branch molecular weight by the entanglement molecular weight M_e then gives the number of entanglement strands.

Figure 8 is a plot of the calculated zero shear viscosity enhancement factors as a function of branch length measured in entanglement strands. An excellent correlation is found for both the four-arm and six-arm PLAs. It is noted that the enhancement grows more rapidly with increasing molecular weight for the six-arm materials than for the four-arm polymers. The enhancement is exponential in arm length as expected from the theoretical treatments discussed next.

E. Star polymer dynamics

The dynamics of star polymers is an area of both theoretical and practical interest. The results presented in Fig. 5 demonstrate the profound nature of the effects on the terminal region upon changing from a linear to a star molecular architecture. This result and other

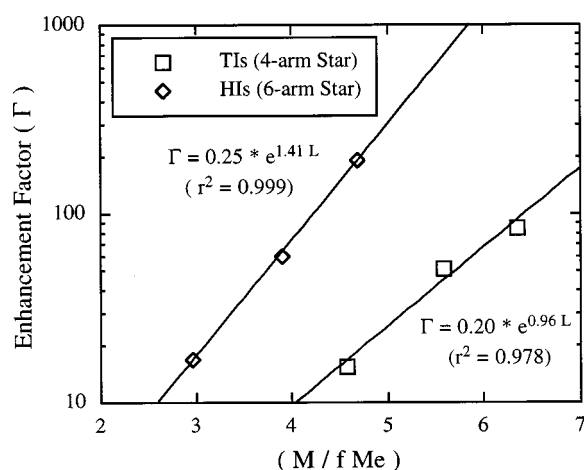


FIG. 8. Viscosity enhancement factors as a function of branching length measured in entanglement strands.

features of the dynamics of star polymers are understandable within the context of hindered reptation [De Gennes (1975)]. In this view the polymer molecule is not free to self-diffuse by reptation because of the constraints placed on the arms by the central branch point. Disentanglement processes are thus dominated by diffusion of the ends of the arms back toward the central star junction. Deep arm retractions are increasingly unlikely as the arm length becomes longer and corresponds to exponentially fewer arm conformations. Arm retraction is therefore a very long relaxation process compared to the reptative relaxation of a linear material. This argument predicts that the zero shear viscosity should increase exponentially, a prediction that is borne out by the experimental facts as evidenced in Fig. 8.

The first comprehensive mathematical treatment of the hindered reptation physical picture is due to Pearson and Helfand and provides a number of additional detailed predictions [Pearson and Helfand (1984)]. These predictions are in accord with the available data on PLA stars. As mentioned above, one distinction between the linear and the star architecture is that the linear material exhibits a maxima in $G''(\omega)$ shortly after passing through the crossover point. In contrast, $G''(\omega)$ continues to increase after the crossover point in both of the star materials (see Figs. 2–4). This behavior is predicted by the Pearson–Helfand theory.

Ball and McLeish extended the arguments of Pearson and Helfand to include the effects of constraint release dynamics [Ball and McLeish (1989)]. Because the relaxation of arm elements near the star core are so much slower than those towards its periphery, the outer chain segments are completely relaxed on the time scale of the more central elements. This relaxation of the peripheral elements introduces a dilution of the entanglement length in the relaxed sections of the molecule. The entanglement length in these regions is divided by the fraction of unrelaxed elements and leads to proportionality between the stress relaxation modulus and the *square* of the unrelaxed path length fraction of the star arm. This contrasts with the first power normally assumed. An additional assumed dilution of the entanglements with unrelaxed volume fraction is motivated by the experimental observation of the scaling of plateau modulus with solvent dilution. These effective reductions in the entanglement structure of the melt are termed “dynamic dilution.” This dilution of the effective entanglements means that the longest relaxations of the star molecules occur more quickly than what is predicted according to the

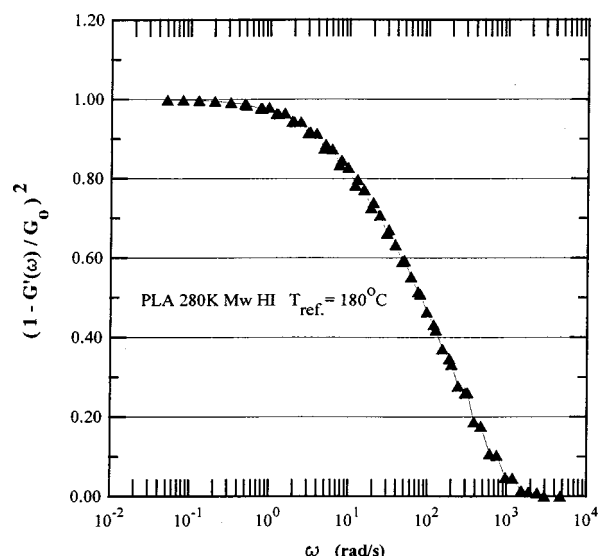


FIG. 9. Plot of $[1 - G'(\omega)/G_n^0]^2$ as a function of logarithmic frequency for a six-arm PLA star polymer. The linearity present is in accordance with the theory of star polymer dynamics.

Pearson–Helfand treatment. In addition, Ball and McLeish examine the effects of polydispersity in their model and find that it can be properly accounted for by simply using the weight average molecular weight as the appropriate measure of molecular size. This latter finding is experimentally relevant and seems to be partially supported by the data presented here.

Milner and McLeish further developed the theory of star polymers [Milner and McLeish (1997)]. In their treatment, higher Rouse modes are considered for short distance arm retractions and the entanglement dilution is taken to go with the volume fraction raised to the four-thirds power. These modifications lead to a theory which can quantitatively describe the dynamics of star polymers given only the plateau modulus, entanglement molecular weight, and Rouse relaxation time for an entanglement strand. These inputs can in principle be determined from data on linear chains. However, quantitative agreement is only expected in the limit of relatively long arms having lengths of more than five entanglement strands.

An additional prediction of the Pearson–Helfand theory is linearity in a plot of $[1 - G'(\omega)/G_n^0]^2$ against the logarithm of frequency. Such a plot is shown in Fig. 9 and does in fact have a large linear region. Similar results are found for the other star polymers providing additional confirmation that the dynamics of PLA star polymers are well described by the concepts present in the theoretical treatment based on the hindered diffusion concept.

However, there is one feature of the above theoretical treatments that is inconsistent with the available experimental data on PLAs. Namely, these theories all predict that for stars with functionalities greater than $f = 3$ (i.e., more than three arms), the zero shear viscosity is dependent only on the arm length and not on the number of arms. This has been found to be true for long arm, monodisperse, polyisoprene star polymers [Fetters *et al.* (1993)]. For these materials, a log–log plot of the zero shear viscosity against the span molecular weight M_s is universal. Polyisoprene star polymers having from 4 to 33 arms all fall on the same curve. The span molecular weight is defined as the longest linear

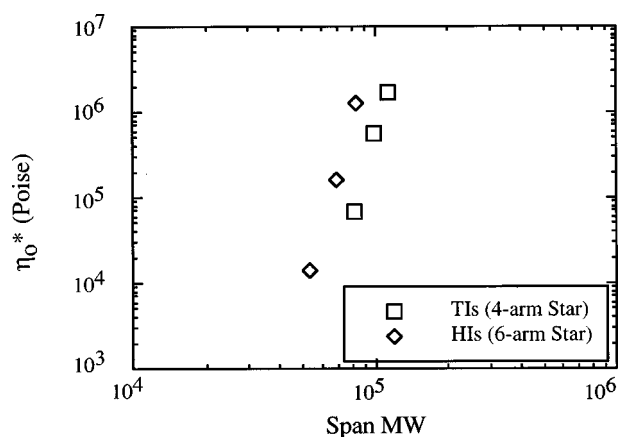


FIG. 10. Zero shear viscosity vs longest linear molecular span. An architectural dependence is evident with the six-arm star exhibiting greater viscosity than the four-arm star for the same arm length.

span in the polymer and for a star is simply twice the arm length. A plot for the PLA stars is shown in Fig. 10. While the data for the two materials certainly do trend together, it is clear that the hexol initiated, six-arm star has a greater viscosity than the tetrol initiated, four-arm star for an equivalent molecular weight.

There are several considerations that could lead to such a discrepancy between the experimental observations and the established theory of star polymer rheology. First, the PLA samples are relatively polydisperse. While the work of Ball and McLeish suggests that mild polydispersity can be accounted for by using the weight average molecular weight, the samples here have polydispersity indexes approaching 2. Thus in comparison to the anionically prepared polyisoprene stars, the PLA stars can be considered very polydisperse. This polydispersity certainly affects the symmetry of the star molecule. Also, while every possible attempt is made to limit the effects of degradation (both by excluding moisture and limiting temperature history), trace reactions can occur. Backbone cleavage would lead to some linear chains being present in the melt. Even trace quantities of such species could profoundly affect the rheological response. The specific stars available have relatively short arm lengths of between three and seven entanglement strands. It should also be remembered that PLA is a relatively stiff polymer that might also take on helical conformations in the melt. Finally, the ester linkages in PLA can participate in hydrogen bonding and such specific interactions may affect arm dynamics. It should be noted though that the trends within a given architecture are very clear despite the polydispersity and other effects. Thus while PLAs are not ideal candidates for critically examining the validity of existing rheological theories, the theories are very useful for explaining many of the observed features of this important class of polymer materials.

V. CONCLUSIONS

Melt rheological properties are of obvious interest if PLA is to become a viable commercial packaging material. In addition, the biomedical importance of PLA warrants a better understanding of its fundamental properties. In this study, these properties are investigated in a comprehensive manner. In particular, entanglement and chain architecture effects on the rheological properties are studied.

For polymers made from a 98:2 ratio of the *L* to *D* enantiomeric monomers it is found that the entanglement molecular weight is approximately 9000 g per mole

($M_e \approx 8700$ g/mol) while the molecular weight for branch entanglement is inferred to be nearly 35 000 g per mole ($M_b \approx 34\,600$ g/mol). In addition, the zero shear viscosity of the linear material apparently increases with molecular weight with the 4.6 power. However, this finding is limited by the small amount of available data (three points) and is subject to considerable experimental uncertainty. An additional finding is that the ratio of the molecular weight for branch entanglement to the entanglement molecular weight is roughly four ($M_b \approx 4M_e$). These results suggest that PLA may be a semistiff polymer possessing a large C_∞ value and characterized by relatively open chain conformations in the melt state.

Viscosity enhancement due to branching in PLAs can be quantified in terms of appropriate enhancement factors. An excellent correlation is found for both four-arm and six-arm PLA stars between viscosity enhancement and branch length measured in entanglement strands.

The dynamics of PLA star architectures are largely described by the theories of Pearson and Helfand, Ball and McLeish, and others. Relaxation spectra show that the transition zone for the linear and branched materials are nearly indistinguishable, while the star polymers have greater contributions to the terminal regime. These and other effects are understandable within the context of a hindered reptation mechanism. The effects of chain architecture on the flow activation are found to be modest, implying that this phenomena is largely controlled by small scale motions in PLA homopolymers. Finally, the zero shear viscosities of PLA star polymers do show some dependence on the number of arms; the six-arm star has a higher melt viscosity than the four-arm star for comparable arm molecular weight. This lack of universality in PLA materials could arise from several sources including polydispersity, hydrogen bonding effects, or the relatively short arm lengths of the specific samples. Despite the lack of universality, arm retraction is still an activated process as demonstrated by the exponential dependence of the viscosity on arm length.

References

- Ball, R. C. and T. C. B. McLeish, "Dynamic Dilution and the Viscosity of Star Polymer Melts," *Macromolecules* **22**, 1911–1913 (1989).
- Cornelis, A. P., H. V. Joziase, D. W. Grijpma, and A. J. Pennings, "On the chain stiffness of poly(lactide)s," *Macromol. Chem. Phys.* **197**, 2219–2229 (1996).
- Datta, R., S. Tsai, P. Bonsignore, S. Moon, and J. R. Frank, "Technological and economic potential of poly(lactic acid) and lactic acid derivatives," *FEMS Microbiol. Rev.* **16**, 221–231 (1995).
- De Gennes, P. G., "Reptation of stars," *J. Phys. (Paris)* **36**, 1199–1203 (1975).
- Dealy, J. M. and K. F. Wissbrun, *Melt Rheology and Its Role in Plastics Processing* (Van Nostrand Reinhold, New York, 1990).
- Ferry, J. D., *Viscoelastic Properties of Polymers* (Wiley, New York, 1980).
- Fetters, L. J., A. D. Kiss, D. S. Pearson, G. F. Quack, and F. J. Vitus, "Rheological behavior of star-shaped polymers," *Macromolecules* **26**, 647–654 (1993).
- Flory, P. J., *Principles of Polymer Chemistry* (Cornell University Press, Ithaca, NY, 1953).
- Graessley, W. W., "Effect of long branches on the flow properties of polymers," *Acc. Chem. Res.* **10**, 332–339 (1977).
- Grijpma, D. W. and A. J. Pennings, "Copolymers of L-lactide, 2. Mechanical properties," *Macromol. Chem. Phys.* **195**, 1649–1663 (1994).
- Grijpma, D. W., J. P. Penning, and A. J. Pennings, "Chain entanglement, mechanical properties and drawability of poly(lactide)," *Colloid Polym. Sci.* **272**, 1068–1081 (1994).
- Jalil, R., "Biodegradable poly(lactic acid) and poly(lactide-co-glycolide) polymers in sustained drug delivery," *Drug Dev. Ind. Pharm.* **16**, 2353–2367 (1990).
- Kohn, J., ed., "Tissue engineering," *MRS Bull.* **21**, 18–19 (1996).

- Leenslag, J. W. and A. J. Pennings, "High-strength fibers by hot drawing of as-polymerized poly(L-lactide)," *Polym. Commun.* **28**, 92–94 (1987).
- Mikos, A. G., M. D. Lyman, L. E. Freed, and R. Langer, "Wetting of poly(L-lactic acid) and poly(DL-lactic-co-glycolic acid) foams for tissue culture," *Biomaterials* **15**, 55–58 (1994).
- Milner, S. T. and T. C. B. McLeish, "Parameter-free theory for stress relaxation in star polymer melts," *Macromolecules* **30**, 2159–2166 (1997).
- Park, T. G., S. Cohen, and R. Langer, "Poly(L-lactic acid)/pluronic blends: Characterization of phase separation behavior, degradation, and morphology and use as protein releasing matrices," *Macromolecules* **25**, 116–122 (1992).
- Park, T. G., S. Cohen, and R. Langer, "Controlled drug delivery using polymer/pluronic blends," USA Patent 5,330,768, Massachusetts Institute of Technology (1994).
- Pearson, D. S. and E. Helfand, "Viscoelastic properties of star-shaped polymers," *Macromolecules* **17**, 888–895 (1984).
- Reed, A. M. and D. K. Gilding, "Biodegradable polymers for use in surgery-poly(glycolic)/poly(lactic acid) homo and copolymers," *Polymer* **22**, 494–498 (1981).
- Sampath, S. S., K. Garvin, and D. H. Robinson, "Preparation and characterization of biodegradable poly(L-lactic acid) gentamicin delivery systems," *Int. J. Pharm.* **78**, 165–174 (1992).
- Siparsky, G. L., K. J. Voorhees, J. R. Dorgan, and K. Schilling, "Water transport in poly(lactic acid), poly(lactic acid-co-caprolactone) copolymers, and poly(lactic acid)/polyethylene glycol blends," *J. Environ. Polym. Degradation* **5**, 125–136 (1997).
- Spinu, M., C. Jackson, M. Y. Keating, and K. H. Gardner, "Material design in poly(lactic acid) systems: Block copolymers, star homo-and copolymers, and stereocomplexes," *J. Macromol. Sci., Pure Appl. Chem.* **A33**, 1497–1530 (1996).
- Sturesson, C., J. Carlfors, K. Edsman, and M. Anderson, "Preparation of biodegradable poly(lactic-co-glycolic acid) microspheres and their in vitro release of timolol maleate," *Int. J. Pharm.* **89**, 235–244 (1993).
- Taylor, M. S., A. U. Daniels, K. P. Andriano, and J. Heller, "Six bioabsorbable polymers: In vitro acute toxicity of accumulated degradation products," *J. Appl. Biomater.* **5**, 151–157 (1994).
- Thayer, A., "Polylactic acid is basis of Dow, Cargill venture," *Chem. Eng. News*, December, 14–16 (1997).
- Tonelli, A. E. and P. J. Flory, "The configurational statistics of random poly(lactic acid) chains. I. Experimental results," *Macromolecules* **2**, 225–227 (1969).
- Tonelli, A. E., P. J. Flory, and D. A. Brandt, "The configurational statistics of random poly(lactic acid) chains. II. Theory," *Macromolecules* **2**, 227–235 (1969).
- Wang, J., R. Kean, J. Randal, and D. Giles, "Melt rheology of polylactide," Society of Rheology Annual Meeting, Columbus, OH, 1997, Poster PO24.
- Witzke, D. R., "Introduction to properties, engineering, and prospects of polylactide polymers," Ph.D. thesis, Chemical Engineering, Michigan State University, 1997.
- Wu, S., "Chain structure and entanglement," *J. Polym. Sci., Part B: Polym. Phys.* **27**, 723–741 (1989).